Journal of Solid State Chemistry 184 (2011) 1946–1950

Contents lists available at ScienceDirect

Journal of Solid State Chemistry

journal homepage: www.elsevier.com/locate/jssc

Structural and optical properties of Ga_2O_3:In films deposited on MgO (1 0 0) substrates by MOCVD

Lingyi Kong, Jin Ma*, Caina Luan, Zhen Zhu

School of Physics, Shandong University, Jinan, Shandong 250100, China

ARTICLE INFO

Article history:
Received 19 October 2010
Received in revised form
20 May 2011
Accepted 29 May 2011
Available online 7 June 2011

Keywords:
Thin film
Oxide
Epitaxy
MgO substrate

ABSTRACT

Ga_2O_3:In films with different indium (In) content x [x=In/(Ga+In) atomic ratio] have been deposited on MgO (1 0 0) substrates by metalorganic chemical vapor deposition (MOCVD). Structural analyses revealed that the film deposited with actual In content (x') of 0.09 was an epitaxial film and the films with x'=0.18 and 0.37 had mixed-phase structures of monoclinic Ga_2O_3 and bixbyite In_2O_3. The absolute average transmittance of the obtained films in the visible region exceeded 95%, and the band gap was in the range of 4.74–4.87 eV. Photoluminescence (PL) measurements were performed at room temperature, in which the visible luminescences were strong and could be seen by the naked eye. The strong emissions in the visible light region were proposed to originate from the gallium vacancies, oxygen deficiencies and other defects in these films.

1. Introduction

Recently, much attention has been focused on the wide band gap oxide semiconductors due to their potential applications in ultraviolet (UV) photodetectors, quantum-well devices and short wavelength light emitting devices. Ga_2O_3 film with the monoclinic structure (β-Ga_2O_3) is a good transparent n-type semiconductor with a wide band gap of about 4.9 eV [1,2]. And this deep-ultraviolet transparent conductive film [3] has been considered as a promising material for a new generation of optoelectronic devices [4–7]. But it presents some difficulties for the Ga_2O_3 film to be used in the construction of various electronic and optical devices. Since the position of conduction band bottom of this material is relatively high, the donor levels tend to become deep levels. So introducing shallow donor levels into this wide band gap semiconductor for release of electrons into the conduction band becomes much more difficult than in most of the narrow band gap semiconductors [3]. According to the theory of Hill [8], similar to the $Mg_xZn_{1-x}O$ ternary compound semiconductor [9–13], Ga_2O_3 could be alloyed with In_2O_3 to tune the band gap of this material. Once Ga_2O_3:In film is available, band gap engineered optoelectronic devices based on this material will have a wide variety of applications.

There have been some reports on the properties of high Ga content Ga–In–O materials [14–19]. Patzke and Binnewies [14] have provided the phase diagram of β-Ga_2O_3/In_2O_3 solid solution system, and high Ga content solid solution of β-$Ga_{2y}In_{2(1-y)}O_3$ ($0.6 \le y \le 1$) has been further studied using Raman spectroscopy by Vigreux et al. [15]. Optical properties of Ga_2O_3-based high Ga content $Ga_{2y}In_{2(1-y)}O_3$ ($0.57 \le y \le 0.96$) films which were prepared by molecular beam epitaxy (MBE) have been studied by Oshim and Fujita [16]. As well as the studies of the Ga–In–O system, $GaInO_3$ film has been used as the active channel material for the transparent thin-film transistors (TTFTs) [17]. However, almost all of the reported high Ga content Ga_2O_3:In films are amorphous or polycrystalline with poor crystalline quality, including the films deposited on yttrium stabilized ZrO_2 (1 0 0) [18] and α-Al_2O_3 (0 0 0 1) [19] substrates by MOCVD. Different from these previous works, epitaxial Ga_2O_3:In films have been deposited on MgO (1 0 0) substrates by MOCVD. Structural and optical properties of the obtained films with different In content ($0.00 \le x' \le 0.37$) have been investigated in detail.

2. Experimental

Ga_2O_3:In films were deposited on MgO (1 0 0) substrates using a high vacuum MOCVD system. The organometallic (OM) sources were commercially available trimethylgallium [$Ga(CH_3)_3$, 6 N in purity] and trimethylindium [$In(CH_3)_3$, 6 N], which were transported into the reactor according to the defined atomic ratio x (experiment desired In content) by ultra high purity N_2 (9 N). And the oxidant which was injected into the reactor was high purity O_2 (5 N) with a flow rate of 50 sccm (sccm denotes cubic centimeter per minute at STP). During the film deposition process,

* Corresponding author. Fax: +86 531 88564886.
E-mail addresses: tongxingzhengkly@163.com (L. Kong), kly2006@mail.sdu.edu.cn (J. Ma), cnluan@mail.sdu.edu.cn (C. Luan), zhuzhen2003@mail.sdu.edu.cn (Z. Zhu).

0022-4596/$ - see front matter © 2011 Elsevier Inc. All rights reserved.
doi:10.1016/j.jssc.2011.05.048

the substrate temperature was kept at 650 °C and the growth pressure at 120 Torr.

The composition and thickness of the films were determined by Rutherford backscattering spectrometry (RBS) using 2.1 MeV He^{2+} ion beam. The crystal structure and the epitaxial relationship of the deposited samples were examined by X-ray diffraction (XRD) and high-resolution transmission electron microscopy (HRTEM). In addition to the $\theta-2\theta$ scans, ω-scan and in-plane Φ-scan were also performed to determine the internal structure of the film. The $\theta-2\theta$ scans were performed using a Bruker D8 Advance X-ray diffractometer with Cu $K\alpha1$ radiation, while the ω-scan and in-plane Φ-scan were performed using a Philips X'Pert Pro MPD X-ray diffractometer with Cu $K\alpha1$ radiation. Cross-section sample was made by gluing two pieces together with thin films facing each other, followed by mechanical polishing and ion milling to obtain a very thin area. Selected area electron diffraction (SAED) and HRTEM were then performed on the sample using a Tecnai F30 transmission electron microscope operated at 300 kV. The optical transmittance spectra were determined using a Shimadzu TV-1900 double-beam UV–vis–NIR spectrophotometer. Also, the PL measurements were performed at room temperature with an SP-2500i fluorescence spectrometer. The excitation light was a pulsed radiation with a wavelength of 266 nm, which was generated by a Ti-sapphire laser (Mira 900-F, Coherent Lasers) pumped with a solid-state laser (Verdi 6, Coherent Lasers).

3. Results and discussion

3.1. Composition and thickness of the films

Fig. 1 shows the RBS spectra of the Ga_2O_3:In films with experiment desired In content $x=0.0$, 0.1, 0.3 and 0.5. The element signals of the samples have been indicated by the arrows in the spectra. The In content and thickness of the Ga_2O_3:In films were calculated from the RBS spectra [20], which have been shown in Table 1. Corresponding to the samples with $x=0.0$, 0.1, 0.3 and 0.5, the calculated In content (x') of the films is 0.00, 0.09, 0.18 and 0.37, respectively. The results show that the actual In content in the films is less than the corresponding experiment desired values, which originates from that $In(CH_3)_3$ predecessor was more easily to be oxidized compared with $Ga(CH_3)_3$ before arriving to the substrates during the deposition process.

3.2. Structural analyses of the films

Fig. 2 shows the XRD spectra of the Ga_2O_3:In films with different In content. Images (a), (b), (c) and (d) correspond to In content x' of 0.00, 0.09, 0.18 and 0.37, respectively. From spectra (a) and (b), the diffraction peaks corresponding to β-Ga_2O_3 (4 0 0), (6 0 0) and (8 0 0) (JCPDS #43-1012) are clearly observed. While in spectra (c) and (d), the bixbyite In_2O_3 (2 2 2) and (4 0 0) (JCPDS #06-0416) peaks emerge. In the meantime, the Ga_2O_3 (8 0 0) peak disappear and the Ga_2O_3 (4 0 0) and (6 0 0) peaks become weak. It can be seen from Fig. 2(a)–(d) that, as In content x' increases

Table 1
In content and thickness of the Ga_2O_3:In films obtained from the RBS spectra.

Sample number	Experiment desired In/(Ga+In) atomic ratio (x)	Calculated In/(Ga+In) atomic ratio (x')	Film thickness (nm)
(a)	0.0	0.00	59
(b)	0.1	0.09	61
(c)	0.3	0.18	40
(d)	0.5	0.37	38

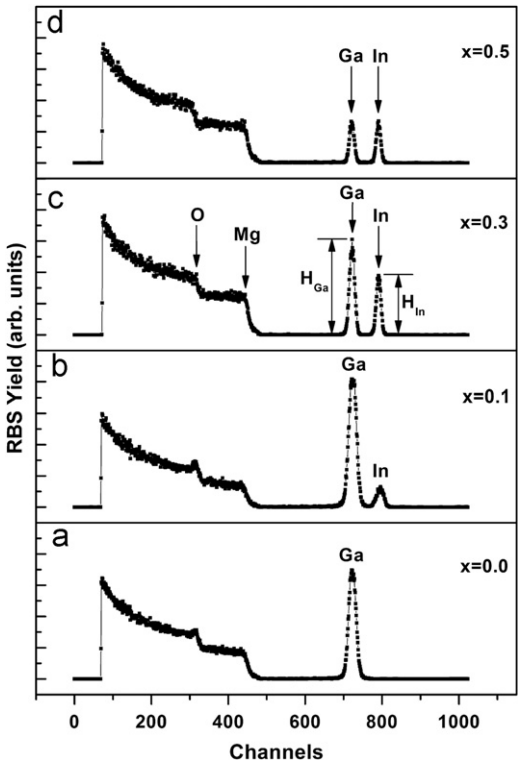

Fig. 1. RBS spectra of the Ga_2O_3:In films with different experiment desired In content x: (a) 0.0, (b) 0.1, (c) 0.3 and (d) 0.5.

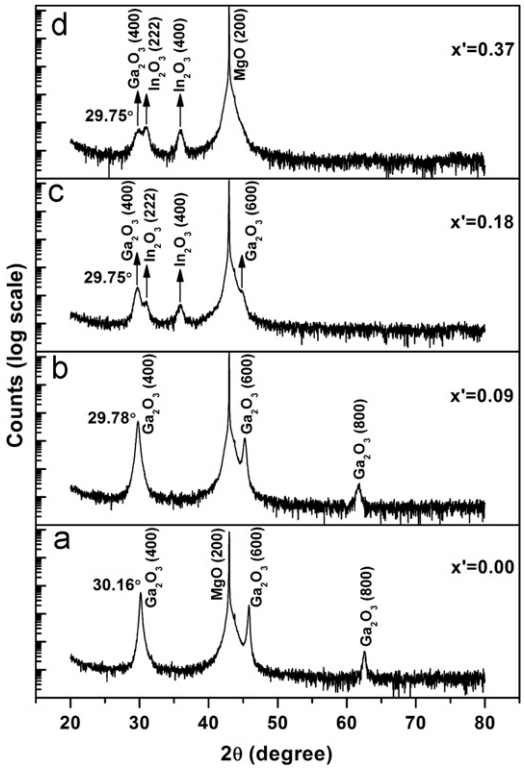

Fig. 2. XRD spectra of the Ga_2O_3:In samples with different actual In content x': (a) 0.00, (b) 0.09, (c) 0.18 and (d) 0.37.

from 0.00 to 0.37, β-Ga_2O_3 diffraction peaks become weaker and polycrystalline In_2O_3 peaks appear and become stronger. Also as the In content x' increases, the diffraction peaks of β-Ga_2O_3 lattice shift to lower angles, such as the location of β-Ga_2O_3 (4 0 0) peak decreases from 30.16° to 29.75°. The interplanar distance of β-Ga_2O_3 (4 0 0) for the samples (a)–(d) can be calculated from the peak location (by Bragg's formula $2d \sin\theta = n\lambda$), which is about 2.961, 2.998, 3.001 and 3.001 Å. Then it can be obtained that the lattice parameter **a** of β-Ga_2O_3 lattice is about 12.19, 12.34, 12.35 and 12.35 Å for the films in (a)–(d), while the standard reference value of undoped β-Ga_2O_3 powder is about 12.23 Å (JCPDS #43-1012). These results originate from that some Ga^{3+} ions in the β-Ga_2O_3 lattice have been replaced by In^{3+} ions. Since the ionic radius of In^{3+} (0.81 Å) is larger than Ga^{3+} (0.62 Å), the interplanar distance becomes larger with increasing In content, which results in the decrease of the Bragg angles. The results also show that, when the In content $x' \geq 0.18$, the Ga_2O_3:In films have mixed structures of β-Ga_2O_3 and polycrystalline In_2O_3 which originate from the phase separation. In addition, all the obtained films show a high resistance property, which is determined by the structure of the films.

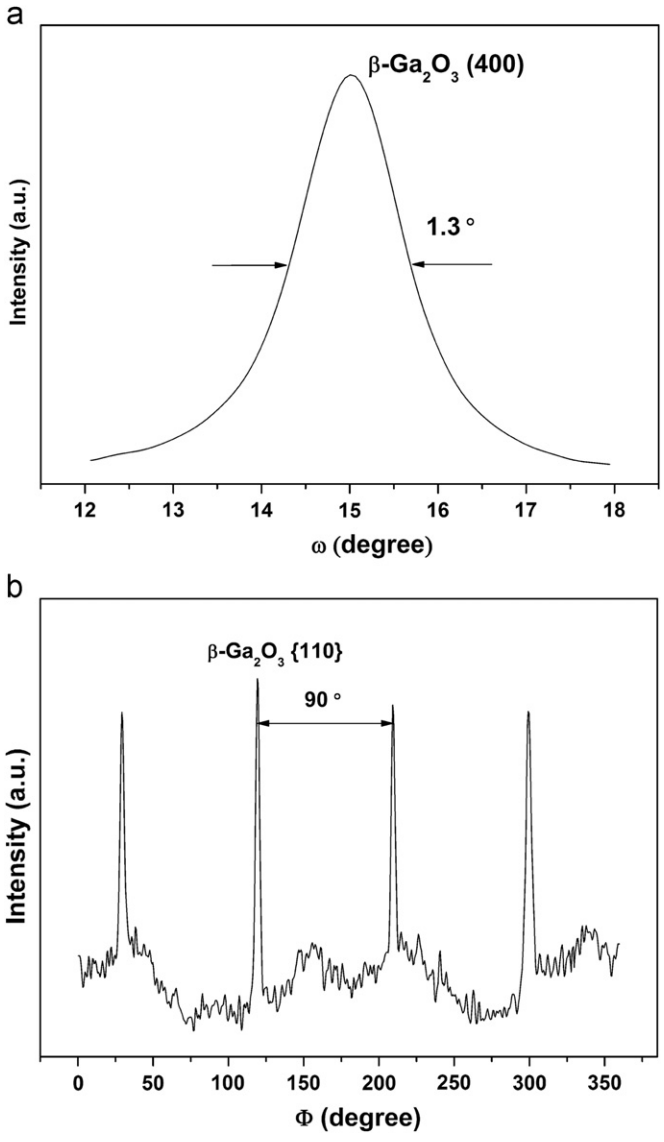

Fig. 3. (a) The ω-rocking curve of β-Ga_2O_3 (400) reflection and (b) the off-specular Φ-scan of β-Ga_2O_3 {1 1 0} planes for the $Ga_{1.82}In_{0.18}O_3$ film.

Fig. 3(a) shows the ω-rocking curve of β-Ga_2O_3 (4 0 0) reflection for the $Ga_{1.82}In_{0.18}O_3$ film, in which a broad full width at half maximum (FWHM) of 1.3° is observed. Fig. 3(b) is the off-specular Φ-scan of β-Ga_2O_3 {1 1 0} planes, showing four diffraction peaks separated by 90°, which reveals a four-domain structure in the $Ga_{1.82}In_{0.18}O_3$ film. The broad FWHM of the ω-rocking curve for β-Ga_2O_3 (400) originates from the crystalline domains inside the film.

Fig. 4(a) shows the low magnification cross-sectional transmission electron microscopy (XTEM) image of the $Ga_{1.82}In_{0.18}O_3$ sample. Fig. 4(b) shows the HRTEM image of the interface area between the $Ga_{1.82}In_{0.18}O_3$ film and MgO substrate, while Fig. 4(c) is the SAED pattern of this interface area. A clear interface between the $Ga_{1.82}In_{0.18}O_3$ film and the MgO substrate can be observed from image (a). From image (b), it can be seen that the deposited $Ga_{1.82}In_{0.18}O_3$ film is an epitaxial film and the growth surface is β-Ga_2O_3 (1 0 0). The SAED pattern of the interface area shows the diffraction spots of Ga_2O_3 (2 0 0), (4 0 0), (6 0 0), (8 0 0), ($\bar{1}$ 1 2) and (5 1 2) planes clearly, in which the diffraction spots of MgO (2 0 0), (0 0 2) and (2 0 2) planes are also clearly observed. The HRTEM and SAED analyses of the interface for the $Ga_{1.82}In_{0.18}O_3$ sample show an epitaxial relationship of $Ga_{1.82}In_{0.18}O_3(1\,0\,0)||MgO(1\,0\,0)$ with $Ga_{1.82}In_{0.18}O_3[0\,0\,1]||MgO\langle 0\,1\,1\rangle$.

3.3. Optical properties

Fig. 5 illustrates the transmittance spectra of the Ga_2O_3:In samples with different In content as a function of wavelength in the range of 200–800 nm. Curves a, b, c and d correspond to In content x' of 0.00, 0.09, 0.18 and 0.37, respectively. The transmittance spectrum of the MgO (1 0 0) substrate (with a thickness of 0.5 mm) is also shown in Fig. 5. The average transmittance of all the samples in the visible wavelength range exceeds 82%, while the MgO substrate has an average transmittance of 86%. The absolute average transmittance (i.e. the substrate contribution is deducted) for the films (38–61 nm thick) in the visible region exceeds 95%.

The optical absorption coefficient (α) and optical band gap (E_g) are related by the following equation [21,22]:

$$\alpha h\nu = A(h\nu - E_g)^{1/2} \quad (1)$$

where h is Planck's constant, ν is the frequency of the incident photon and A is a material dependent constant. The band gap of the obtained films is obtained by plotting $(\alpha h\nu)^2$ vs. $h\nu$ and extrapolating the straight-line portion to the $h\nu$ axis, which is shown in the inset of Fig. 5. The band gap of the films is about 4.87, 4.83, 4.79 and 4.74 eV correspond to In content x' of 0.00, 0.09, 0.18 and 0.37, respectively. These results imply that the Ga_2O_3:In films have excellent transparency and the band gap of the films decreases as the In content increases.

Fig. 6 shows the PL spectra of the Ga_2O_3:In films with different In content as a function of wavelength in the range of 300–800 nm, which were recorded in the same measuring conditions at room temperature (300 K). In these measurements, the spectra were obtained using an average laser power (on the sample) of about 15 mW. Then, the visible luminescences were very strong and could be seen by the naked eye. Curve (a) shows the PL spectrum of the undoped β-Ga_2O_3 film, which is consistent with the reported X-ray and UV excited luminescence spectra of β-Ga_2O_3 single crystals [23], as well as the cathodoluminescence (CL) [24] and PL [25] spectra of β-Ga_2O_3 nanowires. From curve (b), it can be seen that the dominant emissions from the $Ga_{1.82}In_{0.18}O_3$ film are bands located at wavelengths of 439 (2.82 eV) and 417 nm (2.97 eV), different from the spectrum of undoped β-Ga_2O_3 film. The energy band structure was changed by the incorporation of In atoms, but the dominant emissions are also in the blue spectral

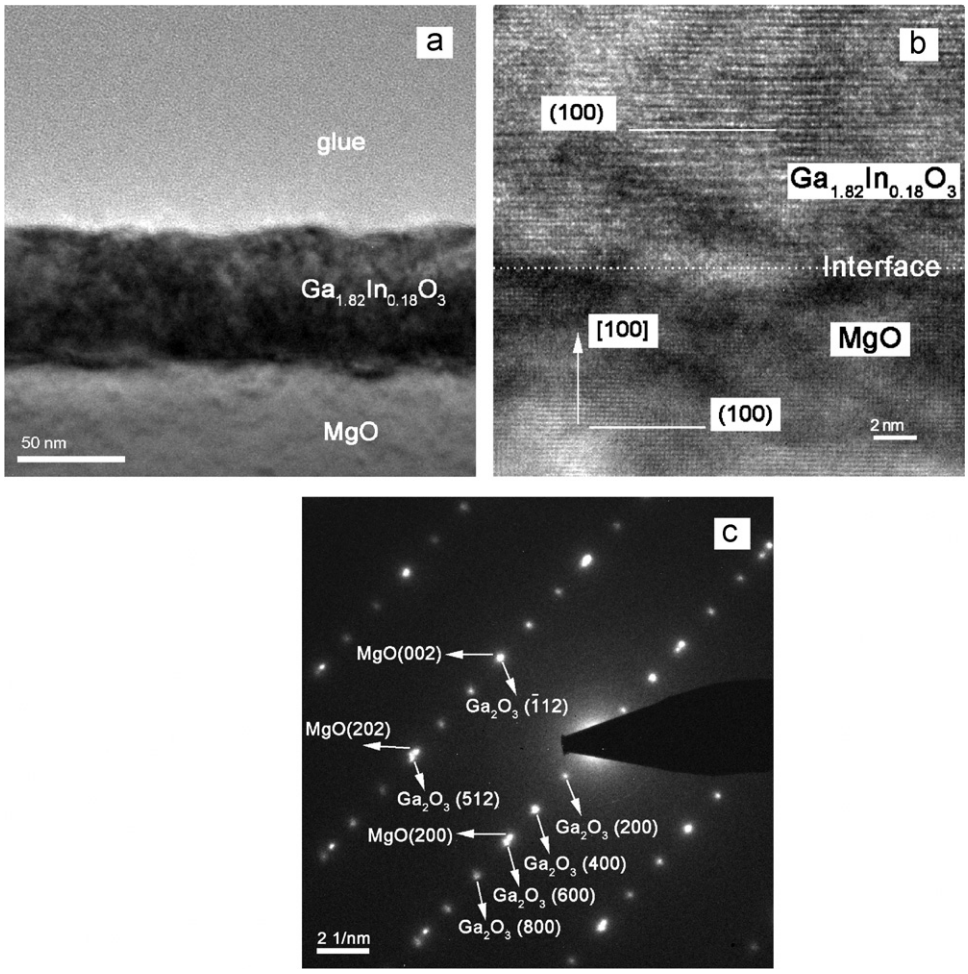

Fig. 4. (a) Low magnification XTEM, (b) HRTEM and (c) SAED micrographs of the interface between the $Ga_{1.82}In_{0.18}O_3$ film and MgO (1 0 0) substrate.

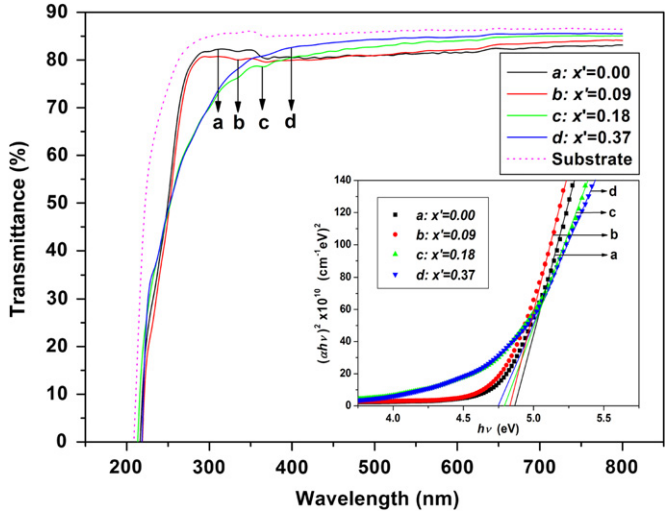

Fig. 5. The transmittance spectra of the Ga_2O_3:In samples: curves a, b, c and d correspond to In content x' of 0.00, 0.09, 0.18 and 0.37, respectively. The inset is the plot of $(\alpha h\nu)^2$ vs. $h\nu$ for the deposited samples.

region. Blue luminescence has been mostly suggested to be produced by a tunneling recombination of an electron on a donor V_o^x with an acceptor which was described as a pair of charged vacancies $(V_o, V_{Ga})'$ [23,24,26–28]. And it has been confirmed that acceptor defects with ground state close to the valence band also participate in the blue emission, which should contain gallium vacancies [26]. Since doping with Si or Zr which increases the concentration of gallium vacancies also enhances the blue luminescence [26,29]. As In content increases in the films, the peak intensity in the visible region shifts to longer wavelengths, which has distinguishable peaks at 494 (2.51 eV) and 510 nm (2.43 eV) with In content x' of 0.18 and 0.37, respectively. The results show that the PL spectra of the Ga_2O_3:In films show a strong dependency on the In content inside the films. The luminescence properties of β-Ga_2O_3 species have been reported [26,27,30] and three characteristic luminescence bands have been observed in the UV (3.40 eV), blue (2.95 eV) and green (2.48 eV) spectral regions [23,26]. And it was reported that the green emission usually occurs in the presence of specific impurities such as Be, Ge and Sn, which has been mostly attributed to the existence of more Ga vacancies in these films [25,29]. We suggest that the emissions in the visible light region originate from the gallium vacancies, oxygen deficiencies and other defects in these films [24,31,32]. The peak location change of the PL spectra caused by the different In content is attributed to the different defect structures in the films, but has not been very clearly understood at this time. Further experiments and systematic studies would be necessary in order to reveal the mechanism of the observed visible emissions in the Ga_2O_3:In films. These optical characteristics of Ga_2O_3:In films will open up new possibilities for application in optoelectronic devices such as visible light sources.

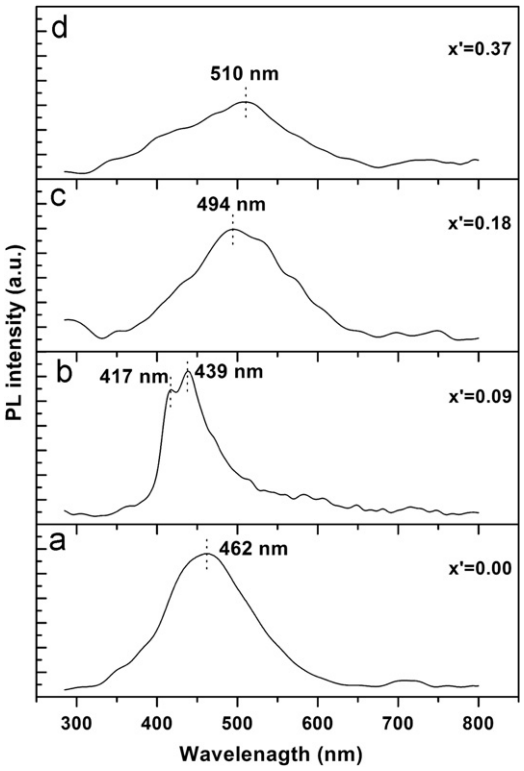

Fig. 6. Room temperature PL spectra of the Ga_2O_3:In films with different In content x': (a) 0.00, (b) 0.09, (b) 0.18 and (c) 0.37.

4. Conclusions

Ga_2O_3:In films with different In content x' ($0.00 \leq x' \leq 0.37$) have been deposited on MgO (1 0 0) substrates at 650 °C by MOCVD. Structural analyses showed that the film with In content x' of 0.09 was an epitaxial film and the growth surface was β-Ga_2O_3 (1 0 0), while the films with x' of 0.18 and 0.37 had mixed structures of β-Ga_2O_3 and polycrystalline In_2O_3. The absolute average transmittance for the obtained films in the visible region exceeded 95%, and the band gap decreased monotonously from 4.87 to 4.74 eV as the In content x' increased from 0.00 to 0.37. In the room temperature PL measurements, strong emissions in the visible light region which originated from the gallium vacancies, oxygen deficiencies and other defects in these films have been observed. The Ga_2O_3:In films may have wide applications in the construction of quantum-well devices, UV photodetectors and short wavelength light emitting devices.

Acknowledgments

This work is financially supported by the National Natural Science Foundation of China (Grant no. 50672054 & 51072102). The authors thank Mr. Z.J. Yin for the PL measurements performed in the Institute of Solid State Physics in Anhui Province of China.

References

[1] F. Zhu, Z. Yang, W. Zhou, Y. Zhang, Appl. Surf. Sci. 252 (2006) 7930.
[2] L. Binet, D. Gourier, C. Minot, J. Solid State Chem. 113 (1994) 420.
[3] M. Orita, H. Ohta, M. Hirano, H. Hosono, Appl. Phys. Lett. 77 (2000) 4166.
[4] G. Sinha, D. Ganguli, S. Chaudhuri, J. Colloid Interface Sci. 319 (2008) 123.
[5] X. Liu, G. Qiu, Y. Zhao, N. Zhang, R. Yi, J. Alloys Compd. 439 (2007) 275.
[6] Q. Xu, S. Zhang, Superlattices Microstruct. 44 (2008) 715.
[7] F. Zhu, Z.X. Yang, W.M. Zhou, Y.F. Zhang, Appl. Surf. Sci. 253 (2006) 1655.
[8] R. Hill, J. Phys. C: Solid State. 7 (1974) 521.
[9] R. Ghosh, D. Basak, Appl. Surf. Sci. 255 (2009) 7238.
[10] W. Wei, C. Jin, J. Narayan, R.J. Narayan, Solid State Commun. 149 (2009) 1670.
[11] R. Ghosh, D. Basak, J. Appl. Phys. 101 (2007) 023507.
[12] I. Takeuchi, W. Yang, K.-S. Chang, M.A. Aronova, T. Venkatesan, R.D. Vispute, L.A. Bendersky, J. Appl. Phys. 94 (2003) 7336.
[13] A. Ohtomo, M. Kawasaki, T. Koida, K. Masubuchi, H. Koinuma, Y. Sakurai, Y. Yoshida, T. Yasuda, Y. Segawa, Appl. Phys. Lett. 72 (1998) 2466.
[14] G. Patzke, M. Binnewies, Solid State Sci. 2 (2000) 689.
[15] C. Vigreux, L. Binet, D. Gourier, B. Piriou, J. Solid State Chem. 157 (2001) 94.
[16] T. Oshima, S. Fujita, Phys. Status Solidi C 5 (2008) 3113.
[17] R.E. Presley, D. Hong, H.Q. Chiang, C.M. Hung, R.L. Hoffman, J.F. Wager, Solid State Electron. 50 (2006) 500.
[18] L. Kong, J. Ma, F. Yang, C. Luan, Z. Zhu, J. Alloys Compd. 499 (2010) 75.
[19] F. Yang, J. Ma, C. Luan, L. Kong, Appl. Surf. Sci. 255 (2009) 4401.
[20] W.K. Chu, J.W. Mayer, M.A. Nicolet, Backscattering Spectrometry, first ed., Academic press, New York, 1978.
[21] K. Jung, W.K. Choi, S.J. Yoon, H.J. Kim, J.W. Choi, Appl. Surf. Sci. 256 (2010) 6219.
[22] R.K. Gupta, K. Ghosh, R. Patel, P.K. Kahol, J. Cryst. Growth 310 (2008) 4336.
[23] E.G. Víllora, K. Hatanaka, H. Odaka, T. Sugawara, T. Miura, H. Fukumura, T. Fukuda, Solid State Commun. 127 (2003) 385.
[24] D.P. Yu, J.L. Bubendorff, J.F. Zhou, Y.L. Wang, M. Troyon, Solid State Commun. 124 (2002) 417.
[25] C.H. Liang, G.W. Meng, G.Z. Wang, Y.W. Wang, L.D. Zhang, S.Y. Zhang, Appl. Phys. Lett. 78 (2001) 3202.
[26] L. Binet, D. Gourier, J. Phys. Chem. Solids 59 (1998) 1241.
[27] V.I. Vasiltsiv, Ya.M. Zakharko, Ya.I. Prim, Ukr. Fiz. Zh. 33 (1988) 1320.
[28] X.C. Wu, W.H. Song, W.D. Huang, M.H. Pu, B. Zhao, Y.P. Sun, J.J. Du, Chem. Phys. Lett. 328 (2000) 5.
[29] T. Harwig, F. Kellendonk, J. Solid State Chem. 24 (1978) 255.
[30] V.I. Vasiltsiv, Ya.M. Zakharko, Sov. Phys. Solid State 25 (1983) 72.
[31] J.H. Hao, J. Gao, Appl. Surf. Sci. 253 (2006) 372.
[32] E.G. Víllora, T. Atou, T. Sekiguchi, T. Sugawara, M. Kikuchi, T. Fukuda, Solid State Commun. 120 (2001) 455.